# Oligomeric hypercomplex of the complete oxidative phosphorylation system in heart mitochondria.

S.V. Nesterov[1,2,*], Yu.M. Chesnokov[3,4], R.A. Kamyshinsky[1,3,4], A.A Panteleeva[5], K.G. Lyamzaev[5], R.G. Vasilov[3], L.S. Yaguzhinsky[1,2,5]

[1] *Moscow Institute of Physics and Techonology, 141701 Dolgoprudny, Moscow Region, Russia*

[2] *Institute of Cytochemistry and Molecular Pharmacology, 115404 Moscow, Russia*

[3] *National Research Center «Kurchatov Institute», 123182 Moscow, Russia*

[4] *Federal Scientific Research Centre "Crystallography and Photonics" of Russian Academy of Sciences, 119333 Moscow, Russia*

[5] *Belozersky Research Institute for Physico-Chemical Biology, Lomonosov Moscow State University, 119992 Moscow, Russia*

* *e-mail: semen.v.nesterov@phystech.edu*

**Abstract**

The existence of a complete oxidative phosphorylation system supercomplex including both electron transport system and ATP synthases has long been assumed based on functional evidence. However, no conclusive structural evidence has been obtained. In this study cryo-electron tomography was used to reveal the supramolecular architecture of the rat heart mitochondria cristae obtained by a mild destruction of mitochondria. For the first time the complete oxidative phosphorylation supercomplexes were observed in mitochondrial membrane under phosphorylating conditions. We show that rows of respiratory chain supercomplexes (respirasomes) are connected with rows of ATP synthases forming the oligomeric hypercomplex. We thus demonstrate that the distance between respirasomes and ATP synthases in hypercomplexes ensures a direct proton transfer from pumps to ATP synthase without proton solvation in the aqueous phase.

## Introduction

Respiratory supercomplexes (respirasomes) in mitochondria are the keystones ensuring the efficient electron transport and no energy leakage. At the same time, the energy transfer to the final stage of oxidative phosphorylation (OXPHOS) system requires the protons rather than electrons. However, despite the evidence on the functional link between proton pumps and ATP synthase has been gained, the existence of complete OXPHOS supercomplexes – hypercomplexes – was questioned. Here, we aim to provide the first experimental evidence on how these hypercomplexes are organized in mitochondria and discuss how they operate.

The existence of respiratory supercomplexes was shown for the first time in bacteria (*1*), and later they were detected in yeast, mammals, and plants by blue-native gel electrophoresis with mild detergents used (*2*, *3*). The method has proved that the long-established functional link between succinate dehydrogenase and ATP synthase (*4*) is a structural docking (*5*). It also confirmed the docking of some mitochondrial dehydrogenases with complex I (*6*), which was previously demonstrated in the isolated enzymes (*7*, *8*). Largely due to the research area focusing on isolating the individual supercomplexes, it became generally accepted that a part of the OXPHOS system can be organized as a supercomplex in many plant and animal species (*9*, *10*).

The existence of stable ATP synthase rows in mitochondrial membranes was previously shown by various methods (*11–13*). The possibility to form linear structures from respirasomes was assumed earlier on the basis of structural analysis (*14*), but it was not proved experimentally. Moreover, there was no experimental evidence of a structural connection between respirasomes and ATP synthases, despite the fact that their coupling was shown functionally (*4*, *15*). All the discovered and previously described OXPHOS supercomplexes can be divided into two groups. The first is called respirasome and includes respiratory chain complexes in different proportions (*16–19*). The second is called ATP-synthasome and includes ATP synthase, phosphate and ADP transporters (*20–22*). The direct

structural coupling of these two subsystems (producer and consumer of protons with excess energy) has not been revealed yet. This work offers a structural solution to this long-standing problem.

## Results

### *Respirasome structure*

The first step of the research included applying cryo-electron tomography (cryo-ET, see Methods) to determine the structure of the rat heart mitochondrial respiratory chain supercomplex. Single-particle cryo-ET (SPT) provides a sufficiently high resolution to identify single proteins in the mitochondrial membrane. The resolution of SPT is limited by the thickness of the sample, therefore, we studied the samples obtained through self-destruction of the rat heart mitochondria isolated by the standard protocol. The diluted mitochondria suspension was kept without substrates for a relatively long time (for more details see Methods). The mitochondria were not exposed to any influences that could have seriously violated their native lipid and protein organization, such as osmotic shock, detergents or centrifugation prior to flash-freezing. After the vitrification procedure, the thinnest areas of the prepared EM grids with fragments of phosphorylating mitochondria, consisting mostly of destroyed mitoplasts and tubular cristae forming a continuous network (Fig. S1), were selected for SPT. The implemented approach allowed to determine different mitochondrial complexes localized in the minimally damaged inner mitochondrial membranes, as well as to obtain their structures with a satisfactory resolution.

The protein composition of respirasome (complexes I, III, IV) and mutual arrangement of its components (Fig. 1) were studied with SPT. The density maps with 27-30 Å spatial resolution were obtained and two types of respirasomes with different number of complexes IV (Fig. S2) were revealed. Comparing the obtained results with blue-native electrophoresis (Fig. S3) and pertinent literature (*16*) indicates that in our samples the structure of supercomplexes is well

preserved. This is confirmed by a much higher relative content of respirasomes containing two complexes IV in our cryo-ET experiments (more than 50%).

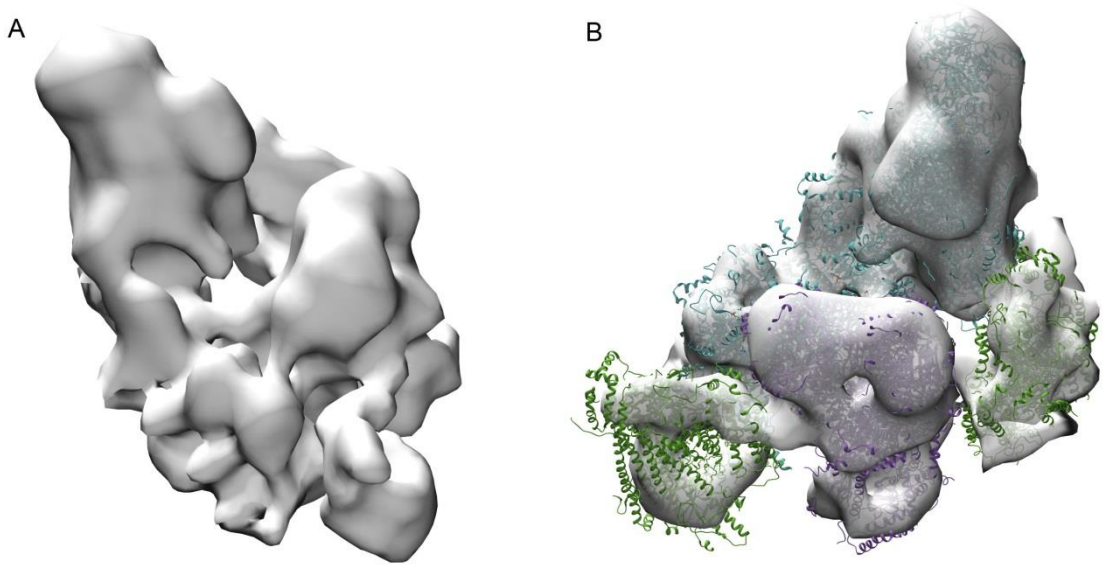


*Fig. 1. A. Cryo-EM map of the most common type of respirasome (mitochondrial respiratory chain supercomplex). B. 90° rotated cryo-EM map with fitted high-resolution structures (PDB 5z62, 5xtd, 1bjy). Blue - complex I, purple - complex III dimer, green - complex IV.*

***The structure of oligomeric OXPHOS hypercomplex***

The second step included studying the supramolecular organization of mitochondrial cristae. It has been shown that under experimental conditions the respirasomes and ATP synthases form highly ordered oligomeric elongated structures – the hypercomplexes (Fig. 2A). The Cryo-ET data demonstrates that linear structures consisting of respirasomes $I_1III_2IV_2$ and $I_1III_2IV_1$ are colocalized with parallel linear structures consisting of ATP synthase oligomers (Fig. 2, 3, S4). The distance between respirasomes and ATP synthases in most of the observed structures is 1-5 nm. It should be emphasized that there are some areas where tight docking of ATP synthases with complexes I or IV (comparable with the distance between complexes in respirasomes) is observed, which makes it possible to consider these areas as canonical supercomplexes of a complete OXPHOS system. It is essential to point out that the elongated transmembrane parts of complexes I

are oriented approximately parallel to the row of ATP synthases, and the complex III dimers are nearly perpendicular to the ATP synthase line. More than that, the line of respirasomes repeats the bend of the ATP synthase line, indicating an interaction that holds these structures together. The Cryo-ET sections and the 3D reconstructions of cristae are shown in the video (movie 1). It should be noted that in all reconstructions only the reliably identified respirasomes and ATP synthases were demonstrated.

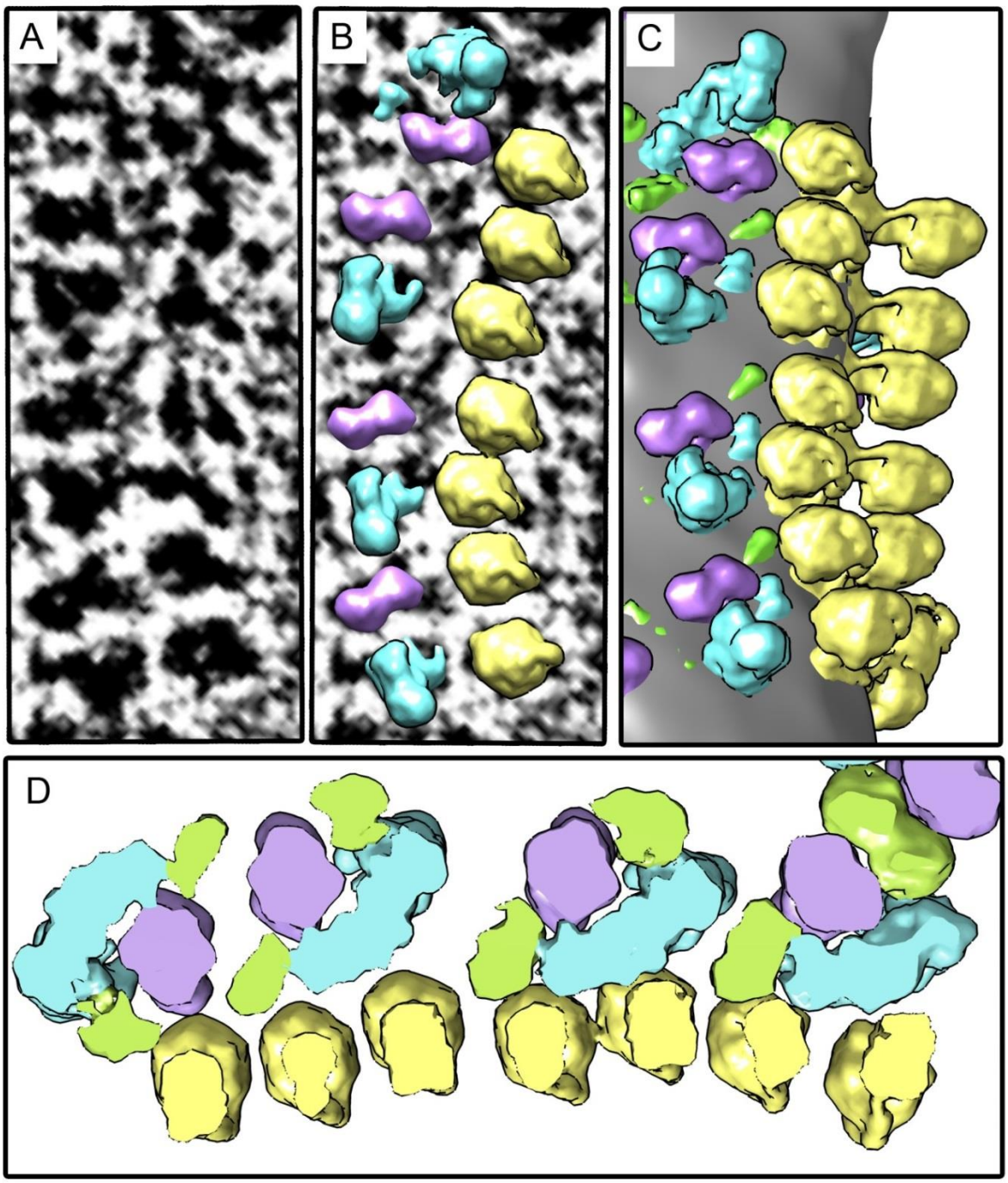

*Fig. 2. An example of oligomeric linear hypercomplex consisting of tightly docked ATP synthases and respirasomes. Elongated transmembrane parts of complexes I are oriented parallel to the row of ATP synthases. A. Tomographic slice. B. Density maps of complexes I, $III_2$ and ATP synthases placed back to the tomogram. C. Surface rendering of the selected area. D. Slice of the density map, view from the intermembrane space. Image D is a bit enlarged in comparison with Fig. A-C. Colors: yellow - ATP synthase, blue - complex I, purple - complex III dimer, green - complex IV.*

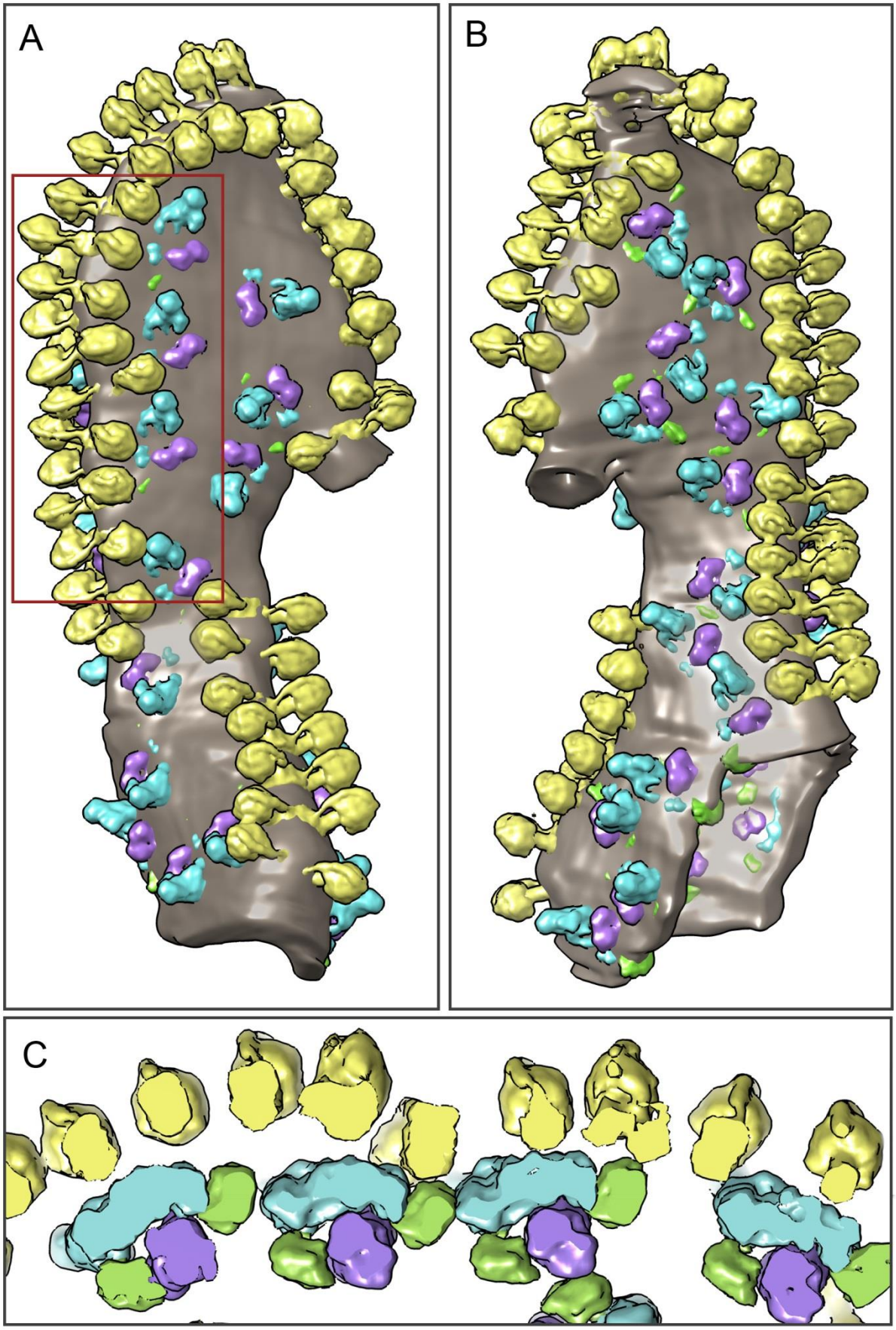
A
B
C

*Fig. 3. Surface rendering of the mitochondrial crista containing the oligomeric linear hypercomplex of the respiratory chain and ATP synthases. A and B. Views of the crista from the opposite sides (180° rotation around the vertical axis), demonstrating a highly ordered structure of the hypercomplex. C. 3D visualization of respirasomes and the ATP synthases contact zones in the membrane. Slice of the fragment highlighted by the red frame in Fig. A. View from the opposite side of the membrane. Colors: yellow - ATP synthase, blue - complex I, purple - complex III dimer, green - complex IV.*

The minimal chain of the OXPHOS supercomplex can be conditionally distinguished from the linear hypercomplexes embracing respirasomes and ATP synthases. It consists of two ATP synthase dimers located on the membrane fold, which are symmetrically docked with the respirasomes at both sides (Fig. S5).

**Discussion**

Cumulatively, our data offer the first structural evidence on the complete OXPHOS supercomplex. Unexpectedly, it turned out that the coupling of proton pumps and ATP synthases occurs not at the level of individual enzymes, but via attraction of large ordered oligomeric structures that results in the formation of hypercomplexes. The existence of these tightly docked structures still raises the question of their functional significance and operation mechanisms to be discussed further. The distinctive peculiarity of the observed structure is that it allows a direct proton transfer from proton pumps to ATP synthase. The basic principles of the detected hypercomplexes' functioning will be briefly summarized below.

The generally accepted OXPHOS model was championed by P. Mitchell (*23*), who proved the proton involvement in OXPHOS, which was later strongly supported by the discovery of an electric field across the mitochondrial membrane made by V. Skulachev and E. Liberman (*24*). However, Mitchell's model assumes the proton departure into the aqueous phase and does not consider the interaction between hydrogen ions and the lipid membrane. This effect was firstly taken into

account in the OXPHOS model proposed by R. Williams (*25*). He proposed that the inner mitochondrial membrane plays the central role in OXPHOS and postulated that the membrane captures hydrogen ions and transfers them to the ATP synthase. Williams' model may be considered as a model of a functional OXPHOS supercomplex with the membrane being an integral part. For a long time, this model remained almost disregarded because the mechanism of proton interaction with the membrane was unelucidated.

The situation changed when the formation of membrane-bound hydrogen ions was detected on the membrane-water interface after transmembrane proton transfer (*26*, *27*). Membrane-bound protons carry free energy excess but do not detach from the membrane due to the existence of kinetic barrier (*26*). That is why the classical uncouplers do not interact with this fraction of protons (*28*). Determining the membrane-bound protons' exact localization (the membrane-water interface) showed that Williams' model may be realized without contradicting Mitchell's main postulate of transmembrane proton transfer. Membrane-bound protons have a high lateral mobility (*29–31*), which enables the energy transfer in the membrane systems without the aqueous phase to be involved. Recently, it was determined that to maintain ATP synthesis in proteoliposomes the distance of proton transfer along the membrane surface should not exceed 80 nm (*32*).

The induction of ATP synthesis on the interface boundary was shown for the first time in the membraneless octane-water model system (*33*). Proton binding at the interface was firstly reported in the biological system during the functioning of rhodopsin proton pumps (*34*). It was also shown that the operation of proton pumps in intact mitochondria and mitochondria without outer membranes leads to the formation of the membrane-bound protons fraction (*35*, *36*). Therefore, the protons with an excess of free energy may be retained on the membrane-water interface and used for ATP synthesis. So, for reaching the maximal efficiency the OXPHOS system should be clustered. The effect of the OXPHOS system clustering was detected in this work.

In the discovered oligomeric hypercomplexes the significant part of respirasomes is tightly docked to ATP synthases. This structure represents the canonical complete OXPHOS supercomplexes. It should be emphasized that the observed hypercomplexes have a highly ordered structure. The other part of respirasomes on cristae is located close enough to ATP synthases for direct proton transfer along the membrane-water interface. These structures correspond to Williams' model of a supercomplex, where the proton-producing system (the respiratory chain) is structurally and functionally connected with the proton-consuming system (the ATP synthase) by the membrane.

It appears that the effectiveness of OXPHOS may be controlled by the transition between a highly ordered oligomeric state with minimal proton leaks and a less ordered diffusely distributed state. However, further research is needed to unveil the mechanisms of this regulation.

## Conclusion

Here a new type of the OXPHOS system structural organization was revealed. It is an oligomeric hypercomplex formed of parallel rows of respirasomes and ATP synthases. The short distance between proton pumps and ATP synthases ensures a direct transfer of membrane-bound hydrogen ions to ATP synthases with minimal leakages. Thus, the discovered hypercomplexes should provide both high efficiency and a high rate of ATP synthesis. These results are in good agreement with the previously found role of the membrane-water interface as a proton accumulator and conductor in the OXPHOS system. The existence of a direct contact between the elements of the hypercomplex should provide not only high energy efficiency but also fast signal transmission for synchronization of the OXPHOS system components.

## References and notes

1. E. A. Berry, B. L. Trumpower, Isolation of ubiquinol oxidase from Paracoccus denitrificans and resolution into cytochrome bc1 and cytochrome c-aa3 complexes. *J. Biol. Chem.* **260**, 2458–2467 (1985).

2. H. Eubel, L. Jänsch, H.-P. Braun, New Insights into the Respiratory Chain of Plant Mitochondria. Supercomplexes and a Unique Composition of Complex II. *Plant Physiol.* **133**, 274–286 (2003).
3. H. Schägger, K. Pfeiffer, Supercomplexes in the respiratory chains of yeast and mammalian mitochondria. *EMBO J.* **19**, 1777–1783 (2000).
4. I. P. Krasinskaya, V. N. Marshansky, S. F. Dragunova, L. S. Yaguzhinsky, Relationships of respiratory chain and ATP-synthetase in energized mitochondria. *FEBS Lett.* **167**, 176–180 (1984).
5. N. Kovářová, T. Mráček, H. Nůsková, E. Holzerová, M. Vrbacký, P. Pecina, K. Hejzlarová, K. Kľučková, J. Rohlena, J. Neuzil, J. Houštěk, High molecular weight forms of mammalian respiratory chain complex II. *PloS One*. **8**, e71869 (2013).
6. Y. Wang, A.-W. Mohsen, S. J. Mihalik, E. S. Goetzman, J. Vockley, Evidence for Physical Association of Mitochondrial Fatty Acid Oxidation and Oxidative Phosphorylation Complexes. *J. Biol. Chem.* **285**, 29834–29841 (2010).
7. Z. Porpaczy, B. Sumegi, I. Alkonyi, Interaction between NAD-dependent isocitrate dehydrogenase, alpha-ketoglutarate dehydrogenase complex, and NADH:ubiquinone oxidoreductase. *J. Biol. Chem.* **262**, 9509–9514 (1987).
8. B. Sumegi, P. A. Srere, Complex I binds several mitochondrial NAD-coupled dehydrogenases. *J. Biol. Chem.* **259**, 15040–15045 (1984).
9. N. V. Dudkina, R. Kouřil, K. Peters, H.-P. Braun, E. J. Boekema, Structure and function of mitochondrial supercomplexes. *Biochim. Biophys. Acta BBA - Bioenerg.* **1797**, 664–670 (2010).
10. D. Milenkovic, J. N. Blaza, N.-G. Larsson, J. Hirst, The Enigma of the Respiratory Chain Supercomplex. *Cell Metab.* **25**, 765–776 (2017).
11. N. Buzhynskyy, P. Sens, V. Prima, J. N. Sturgis, S. Scheuring, Rows of ATP Synthase Dimers in Native Mitochondrial Inner Membranes. *Biophys. J.* **93**, 2870–2876 (2007).
12. P. Paumard, J. Vaillier, B. Coulary, J. Schaeffer, V. Soubannier, D. M. Mueller, D. Brèthes, J.-P. di Rago, J. Velours, The ATP synthase is involved in generating mitochondrial cristae morphology. *EMBO J.* **21**, 221–230 (2002).
13. M. Strauss, G. Hofhaus, R. R. Schröder, W. Kühlbrandt, Dimer ribbons of ATP synthase shape the inner mitochondrial membrane. *EMBO J.* **27**, 1154–1160 (2008).
14. J. B. Bultema, H.-P. Braun, E. J. Boekema, R. Kouril, Megacomplex organization of the oxidative phosphorylation system by structural analysis of respiratory supercomplexes from potato. *Biochim. Biophys. Acta*. **1787**, 60–67 (2009).
15. H. Boumans, L. A. Grivell, J. A. Berden, The Respiratory Chain in Yeast Behaves as a Single Functional Unit. *J. Biol. Chem.* **273**, 4872–4877 (1998).
16. K. M. Davies, T. B. Blum, W. Kühlbrandt, Conserved in situ arrangement of complex I and III2 in mitochondrial respiratory chain supercomplexes of mammals, yeast, and plants. *Proc. Natl. Acad. Sci.* **115**, 3024–3029 (2018).

17. J. Gu, M. Wu, R. Guo, K. Yan, J. Lei, N. Gao, M. Yang, The architecture of the mammalian respirasome. *Nature*. **537**, 639–643 (2016).
18. R. Guo, S. Zong, M. Wu, J. Gu, M. Yang, Architecture of Human Mitochondrial Respiratory Megacomplex I2III2IV2. *Cell*. **170**, 1247-1257.e12 (2017).
19. J. A. Letts, K. Fiedorczuk, L. A. Sazanov, The architecture of respiratory supercomplexes. *Nature*. **537**, 644–648 (2016).
20. C. Chen, Y. Ko, M. Delannoy, S. J. Ludtke, W. Chiu, P. L. Pedersen, Mitochondrial ATP synthasome: three-dimensional structure by electron microscopy of the ATP synthase in complex formation with carriers for Pi and ADP/ATP. *J. Biol. Chem.* **279**, 31761–31768 (2004).
21. Y. Ko, M. Delannoy, J. Hullihen, W. Chiu, P. Pedersen, Mitochondrial ATP synthasome. Cristae-enriched membranes and a multiwell detergent screening assay yield dispersed single complexes containing the ATP synthase and carriers for Pi and ADP/ATP. *J. Biol. Chem.* **278**, 12305–9 (2003).
22. H. Nůsková, T. Mráček, T. Mikulová, M. Vrbacký, N. Kovářová, J. Kovalčíková, P. Pecina, J. Houštěk, Mitochondrial ATP synthasome: Expression and structural interaction of its components. *Biochem. Biophys. Res. Commun.* **464**, 787–793 (2015).
23. P. Mitchell, Coupling of phosphorylation to electron and hydrogen transfer by a chemi-osmotic type of mechanism. *Nature*. **191**, 144–148 (1961).
24. E. A. Liberman, V. P. Topaly, L. M. Tsofina, A. A. Jasaitis, V. P. Skulachev, Mechanism of Coupling of Oxidative Phosphorylation and the Membrane Potential of Mitochondria. *Nature*. **222**, 1076–1078 (1969).
25. R. J. P. Williams, Possible functions of chains of catalysts. *J. Theor. Biol.* **1**, 1–17 (1961).
26. Y. N. Antonenko, O. N. Kovbasnjuk, L. S. Yaguzhinsky, Evidence in favor of the existence of a kinetic barrier for proton transfer from a surface of bilayer phospholipid membrane to bulk water. *Biochim. Biophys. Acta BBA - Biomembr.* **1150**, 45–50 (1993).
27. V. Y. Evtodienko, Y. N. Antonenko, L. S. Yaguzhinsky, Increase of local hydrogen ion gradient near bilayer lipid membrane under the conditions of catalysis of proton transfer across the interface. *FEBS Lett.* **425**, 222–224 (1998).
28. V. I. Yurkov, M. S. Fadeeva, L. S. Yaguzhinsky, Proton transfer through the membrane—water interfaces in uncoupled mitochondria. *Biochem. Mosc.* **70**, 195–199 (2005).
29. S. Serowy, S. Saparov, Y. Antonenko, W. Kozlovsky, V. Hagen, P. Pohl, Structural Proton Diffusion along Lipid Bilayers. *Biophys. J.* **84**, 1031–7 (2003).
30. Y. Antonenko, P. Pohl, Microinjection in combination with microfluorimetry to study proton diffusion along phospholipid membranes. *Eur. Biophys. J. EBJ*. **37**, 865–70 (2008).

31. E. Medvedev, A. Stuchebrukhov, Mechanism of long-range proton translocation along biological membranes. *FEBS Lett.* **587** (2012), doi:10.1016/j.febslet.2012.12.010.
32. J. Sjöholm, J. Bergstrand, T. Nilsson, R. Šachl, C. von Ballmoos, J. Widengren, P. Brzezinski, The lateral distance between a proton pump and ATP synthase determines the ATP-synthesis rate. *Sci. Rep.* **7**, 1–12 (2017).
33. L. S. Yaguzhinsky, L. I. Boguslavsky, A. G. Volkov, A. B. Rakhmaninova, Synthesis of ATP coupled with action of membrane protonic pumps at the octane–water interface. *Nature*. **259**, 494–496 (1976).
34. L. A. Drachev, A. D. Kaulen, V. P. Skulachev, Correlation of photochemical cycle, H+ release and uptake, and electric events in bacteriorhodopsin. *FEBS Lett.* **178**, 331–335 (1984).
35. L. V. Eroshenko, A. S. Marakhovskaya, I. M. Vangeli, P. I. Semenyuk, V. N. Orlov, L. S. Yaguzhinsky, Bronsted Acids Bounded to the Mitochondrial Membranes as a Substrate for ATP Synthase. *Dokl. Biochem. Biophys.* **444**, 158–161 (2012).
36. V. S. Moiseeva, K. A. Motovilov, N. V. Lobysheva, V. N. Orlov, L. S. Yaguzhinsky, The formation of metastable bond between protons and mitoplast surface. *Dokl. Biochem. Biophys.* **438**, 127–130 (2011).
37. H. Schägger, G. von Jagow, Blue native electrophoresis for isolation of membrane protein complexes in enzymatically active form. Anal. Biochem. 199, 223–231 (1991).
38. X. Grandier-Vazeille, M. Guérin, Separation by Blue Native and Colorless Native Polyacrylamide Gel Electrophoresis of the Oxidative Phosphorylation Complexes of Yeast Mitochondria Solubilized by Different Detergents: Specific Staining of the Different Complexes. Anal. Biochem. 242, 248–254 (1996).
39. J. R. Kremer, D. N. Mastronarde, J. R. McIntosh, Computer Visualization of Three-Dimensional Image Data Using IMOD. J. Struct. Biol. 116, 71–76.
40. M. Radermacher, in Electron Tomography, J. Frank, Ed. (Springer New York, New York, NY, 2006; http://link.springer.com/10.1007/978-0-387-69008-7_9), pp. 245–273.
41. D. Kimanius, B. O. Forsberg, S. H. Scheres, E. Lindahl, Accelerated cryo-EM structure determination with parallelisation using GPUs in RELION-2. eLife. 5, e18722 (2016).
42. T. A. M. Bharat, S. H. W. Scheres, Resolving macromolecular structures from electron cryo-tomography data using subtomogram averaging in RELION. Nat. Protoc. 11, 2054–2065 (2016).
43. M. Chen, W. Dai, S. Y. Sun, D. Jonasch, C. Y. He, M. F. Schmid, W. Chiu, S. J. Ludtke, Convolutional neural networks for automated annotation of cellular cryo-electron tomograms. Nat. Methods. 14, 983–985 (2017).
44. J. G. Galaz-Montoya, J. Flanagan, M. F. Schmid, S. J. Ludtke, Single particle tomography in EMAN2. J. Struct. Biol. 190, 279–290 (2015).
45. S. V. Nesterov, Yu. M. Chesnokov, R. A. Kamyshinsky, L. S. Yaguzhinsky, R. G. Vasilov, Nanotechnologies in Russia, in press.

46. E. F. Pettersen, T. D. Goddard, C. C. Huang, G. S. Couch, D. M. Greenblatt, E. C. Meng, T. E. Ferrin, UCSF Chimera - visualization system for exploratory research and analysis. J. Comput. Chem. 25, 1605–1612 (2004).

**Acknowledgments**

This work has been carried out using computing resources of the federal collective usage center Complex for Simulation and Data Processing for Megascience Facilities at NRC “Kurchatov Institute”. **Funding:** This work was supported by the Russian Foundation for Basic Research (grant № 19-04-00835; S.V.N., L.S.Y.) and NRC "Kurchatov Institute" (thematic plan "Study of the processes of generation, transmission and distribution of energy in living organisms"; Y.M.C., R.A.K., R.G.V.). **Author contributions:** L.S.Y., R.G.V. designed the study; S.V.N. and L.S.Y. wrote the manuscript, which was commented on by all authors; S.V.N. performed mitochondria preparation and manual annotation of the tomograms; A.A.P., K.G.L. performed blue-native gel electrophoresis; Y.M.C., R.A.K. performed cryo-EM experiments and computer data processing; **Competing interests:** None declared. **Data and materials availability:** All data are available in the manuscript or the supplementary material.

**Supplementary Materials:**

Materials and Methods

Figures S1-S5

Movie S1

References (37-46)